Preparation and biodistribution study of ^{99m}Tc-EC-Annexin-SPIO as a tracer of radiation induced apoptosis in mice model

Abolghasem Haeri[1], Hossein Rajabi[1], Fariba Johari[2], Shahram Akhlaghpoor[3]

[1]Department of Medical Physics, Faculty of Medical Sciences, Tarbiat Modares University, Tehran, Iran
[2]Department of Radioisotope, Nuclear Science and Technology Research Institute, Tehran, Iran
[3]Department of Radiology, Sina Hospital, Tehran University of Medical Science, Tehran, Iran

ABSTRACT

Introduction: Apoptosis is a major consequence of ionizing radiation in proliferative tissues and quantification of the apoptotic cells could be helpful for noninvasive assessment and estimation of the radiation absorbed dose. Annexin V conjugated with super paramagnetic iron oxide nanoparticles (ANX-SPIO) is a biological probe for detection of apoptotic cells using magnetic resonance imaging. This study aimed at assessing the biodistribution alterations of the labeled ANX-SPIO within the mice body shortly after exposure to different doses of ionizing radiation.

Methods: ^{99m}Tc-EC-ANX-SPIO was prepared and its in vitro stability was tested. The binding affinity of radiocomplex to apoptotic cells was validated in vitro. Mice irradiated whole body with 2, 4 and 6 Gy (^{60}Co gamma rays) and six hours later, radiocomplex was administrated intravenously and the biodistribution study was conducted 0.5, 1 and 2 hours later.

Results: The radiochemical purity of radiocomplex was 94% ± 3.4% and it showed a good stability in PBS and serum. The radiocomplex maintained its efficacy for in vitro binding to apoptotic cells. radiocomplex accumulated in the bone marrow of all irradiated mice (p <0.05). However, statistical analysis did not show significant correlation between the %ID/g of the femoral bones and the received radiation doses.

Conclusion: Quantification of ANX-SPIO in bone marrow can be used as an indicator for radiation exposure but development and optimization of the assay are necessary for discrimination between different radiation doses.

Key words: Radiation; Apoptosis; Annexin V; SPIO; Biodistribution

Corresponding author: Dr Hossein Rajabi, Department of Medical Physics, Faculty of Medical Sciences, Tarbiat Modares University, P.O. Box: 14115331, Tehran, Iran. E-mail: hRajabi@modares.ac.ir

INTRODUCTION

Apoptosis or programmed cell death is critical in many physiologic and pathologic processes [1]. Shortly after exposure to ionizing radiation, apoptosis is a major consequence in the proliferative tissues such as the hematopoietic system [2]. Tracing and quantification of the apoptotic cells could be helpful for noninvasive assessment and rapid estimation of the radiation absorbed dose to the patients [3]. To date, several biochemical features in cells have been identified and used for visualization of apoptosis [4-5]. An early event in apoptosis is translocation of phosphatidylserine from the cytoplasmic face of the membrane to the extracellular domain [6]. Annexin V (ANX), a human protein with a molecular weight of 36 kDa, has a high specific affinity for cells with exposed Phosphatidylserine and suggested as a biological probe for apoptotic cells [7]. ANX has been labeled with different fluorescein for fluorescent detection [8-10], magnetic particles for MRI detection [11-12] and with different radionuclides [3, 13-16] for either single-photon emission computed tomography (SPECT) or positron emission tomography (PET) detection of apoptosis.

Superparamagnetic iron oxide nanoparticle (SPIO) is a highly sensitive magnetite nano cluster for MRI imaging that has many applications in biologic and biomedical studies [17-18]. ANX has been conjugated with SPIO and the sites containing apoptotic cells were detected through negative contrast in T_2 or T_2^* weighted images [19]. MRI has the potential to be used as a noninvasive technique for the detection and measurement of the apoptosis in living tissues [11, 20], but in the irradiated tissues, optimum time of tracer administration after irradiation, MRI imaging time following administration of tracer and target organs must be determined. In the present study, we labeled ANX-SPIO with ^{99m}Tc (^{99m}Tc-EC-ANX-SPIO) followed by administration to whole-body gamma-irradiated normal mice in order to evaluate its biodistribution change after different doses of ionizing radiation. The objective of this study was developing a noninvasive imaging agent for in vivo detection of radiation exposure.

METHODS

Chemicals

ANX-SPIO was obtained from Miltenyi Biotec (Gladbach, Germany). It was consisting of an iron oxide core (size of single iron oxide grains 10 – 12 nm) coated with dextran, conjugated to ANX protein. The concentration of iron and ANX in Miltenyi ANX-SPIO were 0.054 mg and 30 μg per ml respectively [21]. Other chemical agents were supplied from Sigma.

Radiolabeling and radiochemical purity analysis

ANX-SPIO (0.108 mg iron and 60 μg ANX) was chelated with 0.019 mmol ethylenedicysteine (EC), 0.019 mmol N-Hydroxysulfosuccinimide (sulfo-NHS) and 0.019 mmol Ethyl-3-(3-dimethylaminopropyl)-carbodiimide (EDC). The mixture was stirred at room temperature for 24 hrs. After 24 hours, the EC-ANX-SPIO were magnetically separated, re-suspended in PBS (phosphate buffer saline) and stored at 4° C. For radiolabeling, 2 mCi of ^{99m}Tc-pertechnetate and 30 μg $SnCl_2$ were added to 500 μL of EC-ANX-SPIO (Figure 1).

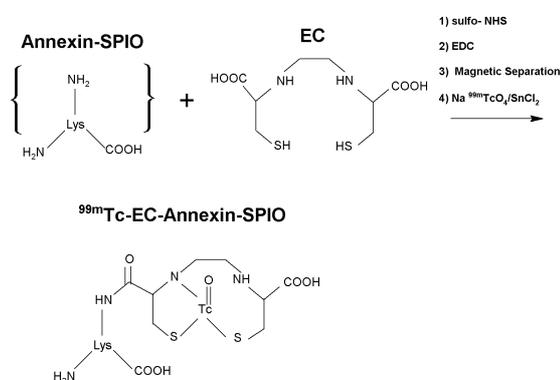**Figure 1.** Synthesis of ^{99m}Tc-EC-ANX-SPIO

Radiochemical purity of the ^{99m}Tc-EC-ANX-SPIO (radiocomplex) was determined by paper chromatography (PC) and thin layer chromatography (TLC) techniques to find out the percentage of reduced radioisotope bound to the radiocomplex and percentage of the free pertechnetate. Whatman paper strips were developed in 100% acetone and the silica gel-coated thin-layer chromatography (TLC-SG) strips in saline.

In vitro stability of the radiocomplex

In vitro stability of radiocomplex was assessed at various time intervals (up to 4 h) in PBS buffer and human blood serum at room temperature. Aliquots of the radiocomplex were applied on Whatman paper and TLC-SG strips. Acetone was used as a mobile phase for PC and saline for TLC. Dissociation of the radiocomplex was determined as the percentage of the free pertechnetate at that time.

In vitro model of apoptosis

Human peripheral blood mononuclear cells (PBMCs) were isolated from the heparinized venous blood of

two healthy volunteers, using density-gradient centrifugation on Ficoll-Hypaque (Lymphoprep, Nyegaard). The PBMCs were washed twice in RPMI 1640 cell culture medium (Gibco, Belgium). PBMCs (1.0×10^6 cells in 1 ml RPMI 1640 culture medium) were irradiated (5 Gy) at 37°C using ^{60}Co source (dose rate 0.5 Gy/min). Control samples (none irradiated cells) and irradiated cells (6 samples in each group) were maintained in RPMI 1640 culture medium for 24 h at 37° C in a 95% air plus 5% CO_2 fully humidified incubator. The culture medium was supplemented with 0.05% L-glutamine, 20 mM HEPES buffer, 50 IU/ml penicillin, 50 mg/ml streptomycin and 15% (v/v) heat inactivated fetal calf serum (Gibco, Scotland) [22].

Binding assay of radiocomplex with apoptotic cells

Cells were withdrawn from culture medium after 24 h of incubation and washed twice with the binding buffer at room temperature. The pellets were re-suspended in the 80 μl of 1 x binding buffer. An aliquot (20 μl) of the radiocomplex was added to the cell suspension and incubated at 6° C for 15 min. Then cells were withdrawn and rinsed three times with the cold binding buffer. The radioactivity in the pellets and supernatants were measured by a well type gamma counter.

Animal model of apoptosis

Swiss male albino mice (20-30 g, 8-10 weeks old, Pasteur Institute, Tehran-Iran) housed in the university animal house with good conditions and given standard mouse pellet and water ad libitum. All animals were kept under controlled lighting conditions (light: dark, 12:12 hours) and temperature (23 ± 2° C).

All the experiments followed a protocol approved by the Institutional Animal Care and Use Committee of the Iranian Institute of Radiological and Medical Sciences. Animals were randomly divided into one control group and three irradiated groups and each group containing nine mice.

Irradiation

Mice were placed in a ventilated Plexiglas cage and irradiated (whole body) with gamma rays (2, 4 and 6 Gy) using a ^{60}Co radiotherapy unit (Theratron, 780C, Canada). The dose rate was 50 cGy/min, the source to subject distance (SSD) was 80 cm and the temperature was ~23°C. After irradiation, mice were returned to the animal house.

Biodistribution study

Six hours after irradiation, mice were injected with 100 μL of radiocomplex (≈120 μCi) via the tail vein

and were sacrificed at 30 min, 1 h and 2 h after injection. Animals were dissected and the brain, liver, heart, lung, stomach, kidney, spleen, intestine, blood and femoral bones were removed quickly. The radioactivity in the tissues was measured using a NaI well type gamma counter. The measured values were corrected for decay and expressed as percent of the injected dose per gram of the tissues (%ID/g).

Statistical analyses

Data were averaged and expressed as mean ± standard deviation (SD). Mann–Whitney U test was used to investigate the possible difference between the groups and p <0.05 were considered statistically significant. Statistical analyses were performed using spss software.

RESULTS

Radiochemical purity and in vitro stability

The radiochemical purity of radiocomplex was 94% ± 3.4% as determined by PC and TLC techniques. The radiocomplex showed a good stability in PBS buffer and human serum at room temperature (Figure 2). The stability of the radiocomplex was 93% ± 3.6% and 88% ± 2.9% in PBS buffer and human blood serum at 4 h, respectively.
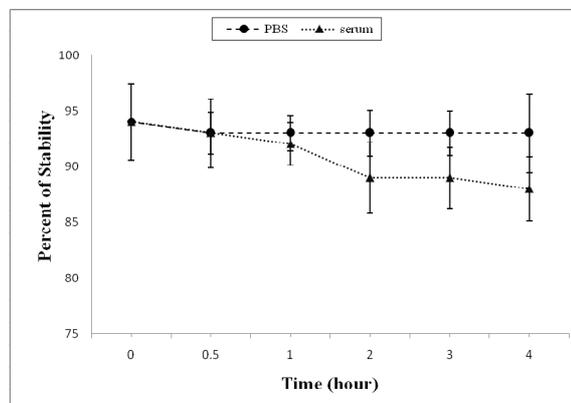

Figure 2. Stability of ^{99m}Tc-EC-ANX-SPIO in phosphate buffered saline and fresh human serum.

Binding affinity of radiocomplex to irradiated cells

The in vitro affinity of radiocomplex for binding to the PBMCs was determined as the activity of the cell pallets after centrifugation. The measured activity was 249 ± 47 and 2263 ± 194 counts per second in non-irradiated and irradiated PBMCs respectively (Figure 3). Comparison of the measured activity clearly showed that radiocomplex retained its

specificity for binding to irradiated apoptotic PBMCs compared to the control PBMCs.
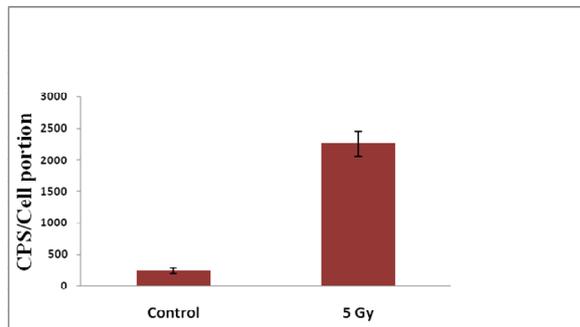

Figure 3. Uptake of ^{99m}Tc-EC-ANX-SPIO by the 5 Gy-irradiated and control lymphocyte (Mean ± SD).

### Biodistribution of radiocomplex in mice

The results of the animal biodistribution studies for radiocomplex in control (non-irradiated), 2 Gy, 4 Gy and 6 Gy irradiated mice are summarized in Figures 4-7, respectively.
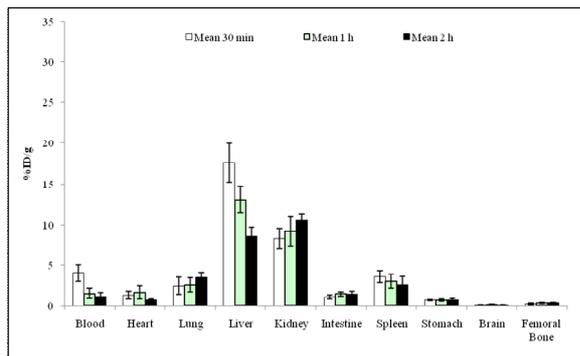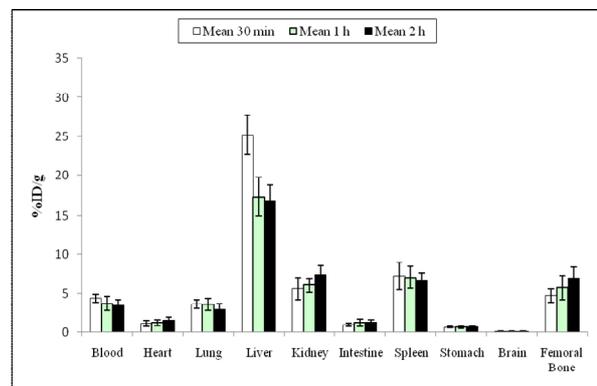

Figure 4. Biodistributions of ^{99m}Tc-EC-ANX-SPIO in control mice (n=3).
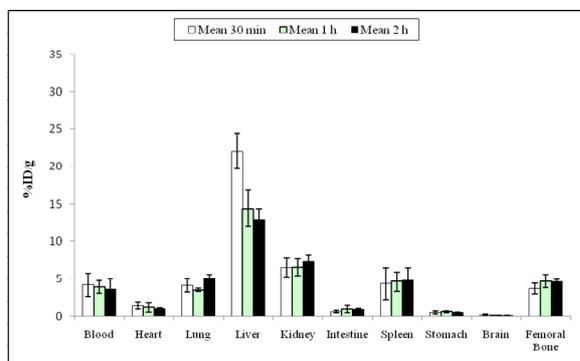
Figure 5. Biodistributions of ^{99m}Tc-EC-ANX-SPIO 6 Hours after whole body irradiation of mice with 2 Gy gamma radiation (n=3).
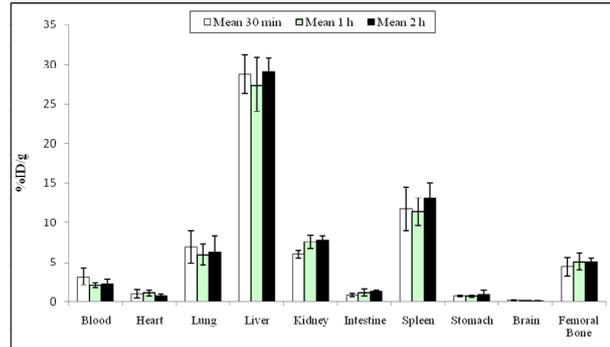
Figure 6. Biodistributions of ^{99m}Tc-EC-ANX-SPIO 6 Hours after whole body irradiation of mice with 4 Gy gamma radiation (n=3).


Figure 7. Biodistributions of ^{99m}Tc-EC-ANX-SPIO 6 Hours after whole body irradiation of mice with 6 Gy gamma radiation (n=3).

The data points are presented as mean ± SD of the calculated %ID/g. In all groups, tracer concentrated primarily in reticuloendothelial system (liver and spleen). The spleen uptake of the radiocomplex in 4 Gy and 6 Gy irradiated mice was remarkably higher than the uptake in control mice at all time points (30 min, 1 h and 2 h) after administration (p < 0.05). Radiocomplex significantly accumulated in the femoral bones of all the irradiated mice as compared to the non-irradiated mice (p < 0.05). However, statistical analysis did not show significant correlation between the %ID/g of the femoral bones and the received radiation doses (Figure 8). On the other hand, the %ID/g of other organs such as intestine, stomach, brain and heart did not show statistically significant differences between the control and irradiated mice (p > 0.05).

DISCUSSION

Tissue damages is a serious complication of exposure to ionizing radiation and finding a suitable imaging agent for noninvasive estimation of absorbed dose has high priority for emergency triage and clinical management of the radiation victims [23].
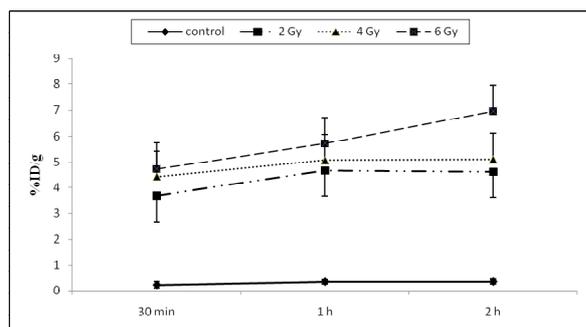
Figure 8. %ID/g of ^{99m}Tc-EC-ANX-SPIO in femoral bones 6 hours after whole body irradiation of mice with different doses of gamma radiation.

As MRI scanners are now available in many general hospitals, finding a new imaging probe that can detect the radiation induced organ or tissue damages prior to the development of severe symptoms is of a critical issue.

In many investigations, ANX has been used for the detection of apoptosis [4]. ANX conjugated with SPIO has already been used as targeting agent for MRI imaging of the apoptotic cells in cardiac tissues through negative contrast in T_2-weighted spin echo images [11, 24-25].

In the present study we radiolabeled the ANX-SPIO as a noninvasive imaging agent for in vivo detection of radiation exposure to living tissues. As the first step, we evaluated the binding ability of radiocomplex to irradiated PBMCs. The measured radioactivity in the 5 Gy irradiated PBMCs was about 9-fold greater than the activity in the control PBMCs. The results clearly showed that radiocomplex maintains its efficacy for binding to apoptotic PBMCs proving the potential capability of the radiocomplex to attach to apoptotic cells.

In order to investigate the capability of the radiocomplex to attach to the apoptotic cells in in-vivo condition we conducted a biodistribution study in the mice that received different doses of ionizing radiation. In the biodistribution study, the irradiated mice presented significantly higher levels of radioactivity in the bone marrows compared to the control mice, showing significant accumulation of radiocomplex in femoral bone marrow even at the low whole body dose of 2 Gy. Therefore ANX-SPIO as apoptosis tracer agent seems to meet the requirement for early detection of radiation-induced bone marrow damage. On the other hand, in order to prove the active accumulation of radiocomplex in bone marrow of the irradiated mice, the biodistribution study of ^{99m}Tc-SPIO without ANX was conducted and the results did not show any accumulation of ^{99m}Tc-SPIO in the bone marrow of the control and irradiated mice (data not shown).

Studies have shown that the percentage of the apoptotic cells increases along with the increase of radiation doses [26-27]. We also observed some increase in the accumulation of the radiocomplex as the radiation dose increased however; statistical analysis did not prove significant relationship between the radiation doses and the %ID/g of the radiocomplex in the bone marrows of the mice (Figure 8).

As most of the ANX-SPIO metabolically accumulates in reticuloendothelial system [28]; so the agent may not be suitable for evaluating the tissue apoptosis of abdominal organs. Recently, ^{99m}Tc-his$_6$-annexin A5 with low accumulation in reticuloendothelial system is proposed as an imaging probe for the abdominal organs shortly after high radiation dose [3].

The sensitivity to radiation and the time for maximum apoptosis varies in different tissues. In vivo apoptotic cells are engulfed by phagocytosis and broken down in the late stage of apoptosis, which may confound in vivo tracing of the apoptotic cells [13]. Since in proliferative tissues, apoptosis occurs shortly after radiation, thus we have selected 6 hours post irradiation for administration of the tracer. It has been shown that in highly proliferated normal tissues such as bone marrow, maximum apoptosis occurs in few hours after radiation and rapidly decreases as the time passing by [29]. Thus, one of the major drawbacks for in vivo tracing of apoptosis is transient nature of this phenomenon and the time of tracer administration after radiation exposure is an important factor that affects the results. Administration of tracer in different times after irradiation should be tested for effectiveness of the assay.

CONCLUSION

In summary, Quantification of ANX-SPIO in bone marrow can be used as an indicator for radiation exposure but development and optimization of the assay are necessary for discrimination between different radiation doses.

Acknowledgements

REFERENCES

1. Blankenberg FG, Katsikis PD, Tait JF, Davis RE, Naumovski L, Ohtsuki K, Kopiwoda S, Abrams MJ, Strauss HW. Imaging of apoptosis (programmed cell death) with 99mTc annexin V. J Nucl Med. 1999 Jan;40(1):184-91.

2. Story MD, Voehringer DW, Malone CG, Hobbs ML, Meyn RE. Radiation-induced apoptosis in sensitive and resistant cells isolated from a mouse lymphoma. Int J Radiat Biol. 1994 Dec;66(6):659-68.

3. Lin KJ, Wu CC, Pan YH, Chen FH, Fu SY, Chiang CS, Hong JH, Lo JM. In vivo imaging of radiation-induced tissue apoptosis by (99m)Tc(I)-his (6)-annexin A5. Ann Nucl Med. 2012 Apr;26(3):272-80.

4. Strauss HW, Blankenberg F, Vanderheyden JL, Tait J. Translational imaging: Imaging of apoptosis. In: München FH. Handbook of experimental pharmacology. Heidelberg: Springer-Verlag Berlin Heidelberg; 2008. p. 259-75.

5. Blankenberg FG. In vivo detection of apoptosis. J Nucl Med. 2008 Jun;49 Suppl 2:81S-95S.

6. Verhoven B, Schlegel RA, Williamson P. Mechanisms of phosphatidylserine exposure, a phagocyte recognition signal, on apoptotic T lymphocytes. J Exp Med. 1995 Nov 1;182(5):1597-601.

7. Blankenberg FG, Katsikis PD, Tait JF, Davis RE, Naumovski L, Ohtsuki K, Kopiwoda S, Abrams MJ, Darkes M, Robbins RC, Maecker HT, Strauss HW. In vivo detection and imaging of phosphatidylserine expression during programmed cell death. Proc Natl Acad Sci U S A. 1998 May 26;95(11):6349-54.

8. Zhang R, Lu W, Wen X, Huang M, Zhou M, Liang D, Li C. Annexin A5-conjugated polymeric micelles for dual SPECT and optical detection of apoptosis. J Nucl Med. 2011 Jun;52(6):958-64.

9. Yang SK, Attipoe S, Klausner AP, Tian R, Pan D, Rich TA, Turner TT, Steers WD, Lysiak JJ. In vivo detection of apoptotic cells in the testis using fluorescence labeled annexin V in a mouse model of testicular torsion. J Urol. 2006 Aug;176(2):830-5.

10. Vermes I, Haanen C, Steffens-Nakken H, Reutelingsperger C. A novel assay for apoptosis. Flow cytometric detection of phosphatidylserine expression on early apoptotic cells using fluorescein labelled Annexin V. J Immunol Methods. 1995 Jul 17;184(1):39-51.

11. Dash R, Chung J, Chan T, Yamada M, Barral J, Nishimura D, Yang PC, Simpson PC. A molecular MRI probe to detect treatment of cardiac apoptosis in vivo. Magn Reson Med. 2011 Oct;66(4):1152-62.

12. Sosnovik DE, Nahrendorf M, Weissleder R. Molecular magnetic resonance imaging in cardiovascular medicine. Circulation. 2007 Apr 17;115(15):2076-86.

13. Khoda Me, Utsunomiya K, Ha-Kawa S, Kanno S, Kono Y, Sawada S. An investigation of the early detection of radiation induced apoptosis by 99mTc-Annexin V and 201thallium-chloride in a lung cancer cell line. J Radiat Res. 2012;53(3):361-7.

14. Kurihara H, Yang DJ, Cristofanilli M, Erwin WD, Yu DF, Kohanim S, Mendez R, Kim EE. Imaging and dosimetry of 99mTc EC annexin V: preliminary clinical study targeting apoptosis in breast tumors. Appl Radiat Isot. 2008 Sep;66(9):1175-82.

15. Cauchon N, Langlois R, Rousseau JA, Tessier G, Cadorette J, Lecomte R, Hunting DJ, Pavan RA, Zeisler SK, van Lier JE. PET imaging of apoptosis with (64)Cu-labeled streptavidin following pretargeting of phosphatidylserine with biotinylated annexin-V. Eur J Nucl Med Mol Imaging. 2007 Feb;34(2):247-58.

16. Murakami Y, Takamatsu H, Taki J, Tatsumi M, Noda A, Ichise R, Tait JF, Nishimura S. 18F-labelled annexin V: a PET tracer for apoptosis imaging. Eur J Nucl Med Mol Imaging. 2004 Apr;31(4):469-74.

17. Lee CM, Jeong HJ, Kim EM, Kim DW, Lim ST, Kim HT, Park IK, Jeong YY, Kim JW, Sohn MH. Superparamagnetic iron oxide nanoparticles as a dual imaging probe for targeting hepatocytes in vivo. Magn Reson Med. 2009 Dec;62(6):1440-6.

18. Andersen LB, Frayne R. Applications of molecular imaging with MR. In: Hallgrímsson CWSaB, editor. Advanced imaging in biology and medicine: Springer-Verlag Berlin Heidelberg; 2009. p. 363-393.

19. Kettunen M, Brindle K. Apoptosis detection using magnetic resonance imaging and spectroscopy. Prog Nucl Mag Reson Spectrosc. 2005;47:175-85.

20. Zhao M, Beauregard DA, Loizou L, Davletov B, Brindle KM. Non-invasive detection of apoptosis using magnetic resonance imaging and a targeted contrast agent. Nat Med. 2001 Nov;7(11):1241-4.

21. Ahrens ET, Feili-Hariri M, Xu H, Genove G, Morel PA. Receptor-mediated endocytosis of iron-oxide particles provides efficient labeling of dendritic cells for in vivo MR imaging. Magn Reson Med. 2003 Jun;49(6):1006-13.

22. Wilkins RC, Kutzner BC, Truong M, Sanchez-Dardon J, McLean JR. Analysis of radiation-induced apoptosis in human lymphocytes: flow cytometry using Annexin V and propidium iodide versus the neutral comet assay. Cytometry. 2002 May 1;48(1):14-9.

23. Pellmar TC, Rockwell S; Radiological/Nuclear Threat Countermeasures Working Group. Priority list of research areas for radiological nuclear threat countermeasures. Radiat Res. 2005 Jan;163(1):115-23.

24. Thorek DL, Chen AK, Czupryna J, Tsourkas A. Superparamagnetic iron oxide nanoparticle probes for molecular imaging. Ann Biomed Eng. 2006 Jan;34(1):23-38.

25. Wolters SL, Corsten MF, Reutelingsperger CP, Narula J, Hofstra L. Cardiovascular molecular imaging of apoptosis. Eur J Nucl Med Mol Imaging. 2007 Jun;34 Suppl 1:S86-98.

26. Paris F, Fuks Z, Kang A, Capodieci P, Juan G, Ehleiter D, Haimovitz-Friedman A, Cordon-Cardo C, Kolesnick R. Endothelial apoptosis as the primary lesion initiating intestinal radiation damage in mice. Science. 2001 Jul 13;293(5528):293-7.

27. Liu WC, Wang SC, Tsai ML, Chen MC, Wang YC, Hong JH, McBride WH, Chiang CS. Protection against radiation-induced bone marrow and intestinal injuries by Cordyceps sinensis, a Chinese herbal medicine. Radiat Res. 2006 Dec;166(6):900-7.

28. Smith BR, Heverhagen J, Knopp M, Schmalbrock P, Shapiro J, Shiomi M, Moldovan NI, Ferrari M, Lee SC. Localization to atherosclerotic plaque and biodistribution of biochemically derivatized superparamagnetic iron oxide nanoparticles (SPIONs) contrast particles for magnetic resonance imaging (MRI). Biomed Microdevices. 2007 Oct;9(5):719-27.

29. Meyn RE, Milas L, Ang KK. The role of apoptosis in radiation oncology. Int J Radiat Biol. 2009 Feb;85(2):107-15.